

# Wave patterns within the generalized convection–reaction–diffusion equation<sup>1</sup>

V. Vladimirov<sup>2</sup>

*Faculty of Applied Mathematics  
University of Science and Technology  
Mickiewicz Avenue 30, 30-059 Kraków, Poland*

**Abstract.** A set of travelling wave solutions to a hyperbolic generalization of the convection–reaction–diffusion is studied by the methods of local nonlinear analysis and numerical simulation. Special attention is paid to displaying appearance of the compactly supported solutions, shock fronts, soliton-like solutions and peakons

**PACS codes:** 02.30.Jr; 47.50.Cd; 83.10.Gr

**Keywords:** generalized convection–reaction–diffusion equation, compactons, peakons, shock fronts, soliton-like travelling wave solutions

## 1 Introduction

As is well-known, there do not exist methods of obtaining the general solutions to most of non-linear evolutionary PDEs. Very often in such circumstances the only alternative to numerical studies of nonlinear models deliver the symmetry-based methods [1]. An important sub-class of the self-similar solutions is formed by the travelling wave (TW) solutions. The object of this study is to demonstrate the existence of a number of localized self-similar TW solutions, basing on the hyperbolic generalization of the convection–reaction–diffusion equation. We pay special attention to the existence of solitary waves [2], shock fronts [3] and some other generalized solutions, such as compactons and peakons [4, 5, 6]. The structure of the study is following. In section 2 we introduce our model equation and next factorize it to an ODE, describing the set of TW solutions. Next we discuss the geometric interpretation of solitary waves and outline the way of capturing them. In sections 3 and 4 we perform the local nonlinear analysis of the dynamical system, equivalent to the factorized ODE, purposed at stating conditions of the wave patterns occurrence. In section 5, we present the results of numerical study, revealing the presence of all above mentioned types of TW solutions. Finally, in section 6, we discuss the results obtained and outline the ways of further investigations.

---

<sup>1</sup>The research was supported by the AGH local grant

<sup>2</sup>*E-mail address:* vsevolod.vladimirov@gmail.com

## 2 Statement of the problem

We consider the following evolutionary equation (referred to as GBE):

$$\alpha u_{tt} + u_t + u u_x - \varkappa (u^n u_x)_x = (u - U_1) \varphi(u). \quad (1)$$

Here  $n$ ,  $\varkappa$ ,  $U_1$  are positive constants,  $\alpha$  is nonnegative. Equation (1) is a generalization of both Burgers equation and the reaction-diffusion equation. Let us note, that the term  $\alpha u_{tt}$  appears when the memory effects are taken into account [8, 9, 10, 11]. Some particular cases of equation (1) were studied in recent years [12, 13, 14, 15, 11, 16]. Owing to these studies, the analytical description of a large variety of travelling wave (TW) solutions is actually available.

Present investigations are mainly devoted to the qualitative and numerical study of the family of TW solution to GBE. Our aim is to show that under certain conditions the set of TW solutions contains solitons, compactons, peakons and some other wave patterns. To put it briefly, we maintain the notation traditionally used in more specific sense. Thus, soliton is usually associated with the exponentially localized invariant TW solution to a completely integrable equations, possessing a number of unusual features [2]. Some of these features are also inherited by the compactons [17, 18]. We maintain the notion to those solutions to (1), which manifest similar geometric features as "true" wave patterns, known under these names.

Let us consider the set of TW solutions

$$u(t, x) = U(\xi) \equiv U(x - Vt). \quad (2)$$

Inserting ansatz (2) into the GBE, one can obtain, after some manipulation, the following dynamical system:

$$\Delta(U) \dot{U} = \Delta(U) W,$$

$$\Delta(U) \dot{W} = (U - V) W - \varkappa n U^{n-1} W^2 - \varphi(U) (U - U_1)$$

where  $\Delta(U) = \varkappa U^n - \alpha V^2$ . By analyzing the factorized system (3), we are going to formulate the conditions contributing to the appearance of the soliton-like solutions and the solutions with compact support, called *compactons*, and some types of generalized TW solutions. Analysis carried out, e.g. in [5, 7] shows, that homoclinic trajectories bi-asymptotic to saddle points correspond to both soliton-like and compacton-like solutions. In the first case the homoclinic loop is bi-asymptotic to a simple saddle, hence, the "time" which is necessary to penetrate such trajectory is infinite. The closed loop representing the compacton is bi-asymptotic to a topological saddle. As a result, the "time" of penetration is finite. In fact, the compacton is a compound generalized solution. Its compactly supported nonzero part corresponds to the closed loop, while the rest corresponds to the stationary point.

In order to "capture" the homoclinic trajectory among the other solutions to the system (3), we are going to state the condition, which guarantee the stable limit cycle appearance. Choice of such strategy is based upon the well-known fact that the growth

of the radius of the limit cycle in presence of a nearby saddle point most often leads to the homoclinic bifurcation. Application of this prescription to the system (3) occurs to have some peculiarities, which are characterized below.

1. The most natural parameter of the bifurcation is the wave pack velocity  $V$ . Yet its change causes the movement of the line of singular points  $\Delta(U) = 0$  (singular line for brevity) in the horizontal direction. As will be shown below, the presence of the topological saddle in most cases is due to the fact that the saddle point belongs to the singular line. On account of this, the problem of "capturing" the compacton-like solution becomes more complicated, for one must "synchronize" the moment of the homoclinic bifurcation with the passage of the singular line through the saddle point.
2. Presence of the singular line delivers an extra mechanism of the limit cycle destruction, competing with the mechanism based upon the homoclinic loop formation.
3. When the far end of the limit cycle approaches the singular line just at the moment of the homoclinic loop formation, the latter becomes flat and reminds triangle. Such loop corresponds to a different type of the generalized solutions, called *peakons* [5, 6].
4. The singular line is unmovable when  $\alpha = 0$ . In this case, corresponding to the parabolic-type model, the analysis becomes much more easy, [19].

### 3 Andronov–Hopf bifurcation in the system (3)

The homoclinic bifurcation can occur in the system (3) if it has an extra stationary point. The function

$$\varphi(U) = (U - U_0)^m \psi(U), \quad 0 \leq U_0 < U_1,$$

considered throughout the remaining part of the work, assures the required geometric configuration, providing that  $\psi(U)$  does not change sign within the segment  $[U_0, U_1]$ .

To formulate the conditions which guarantee the limit cycle appearance in vicinity of the stationary point  $(U_1, 0)$ , let us consider the Jacobi matrix

$$J_1 = \begin{pmatrix} 0 & \Delta(U_1) \\ -\varphi(U_1) & U_1 - V \end{pmatrix}.$$

In order that  $(U_1, 0)$  be a center, the eigenvalues of  $J_1$  should be pure imaginary. This is so if the conditions

$$\text{Trace } J_1 = U_1 - V = 0, \tag{3}$$

$$\text{Det } J_1 = \Delta(U_1) (U_1 - U_0)^m \psi(U_1) > 0 \tag{4}$$

are fulfilled. The first condition immediately gives us the critical value of the wave pack velocity  $V_{cr1} = U_1$ . The second one is equivalent to the statement that both  $\Delta(U_1)$  and  $\psi(U_1)$  are nonzero and have the same signs.

The next thing we are going to do is a study of the stability of the limit cycle. As is well known [20, 21], this is the real part of the first Floquet index  $\Re C_1$  that determines the stability of the periodic trajectory. Depending on the sign of  $\Delta(U_1)$ , there are two possibilities. If  $\Delta(U_1) > 0$  when  $V = V_{cr1}$  or, in other words, the horizontal coordinate of the singular line  $\Delta(U_*) = 0$ , corresponding to the critical value of the parameter  $V$ , satisfies the inequality

$$U_*(V_{cr1}) = \left[ \frac{\alpha V_{cr1}^2}{\varkappa} \right]^{\frac{1}{n}} < U_1,$$

then conditions  $\psi(U_1) > 0$ , and  $\Re C_1 < 0$  should be fulfilled. In case when  $U_*(V_{cr1}) > U_1$ , these parameters should have the opposite signs.

To obtain the expression for  $\Re C_1$ , the standard formula contained e.g. in [21] can be directly applied, provided that our system is presented in the following form:

$$\begin{pmatrix} \dot{z}_1 \\ \dot{z}_2 \end{pmatrix} = \begin{pmatrix} 0 & -\Omega \\ \Omega & 0 \end{pmatrix} \cdot \begin{pmatrix} z_1 \\ z_2 \end{pmatrix} + \begin{pmatrix} F(z_1, z_2) \\ G(z_1, z_2) \end{pmatrix}, \quad (5)$$

where  $\Omega = \sqrt{\mu \cdot \nu}$ ,  $\mu = |\Delta(U_1)|$ ,  $\nu = |\varphi(U_1)|$ ,  $F(z_1, z_2)$  and  $G(z_1, z_2)$  stand for nonlinear terms. In this (canonical) representation  $\Re C_1$  is expressed as follows [21]:

$$16 \Re C_1 = F_{111} + F_{122} + G_{112} + G_{222} + \frac{1}{\Omega} \{ F_{12} (F_{11} + F_{22}) - G_{12} (G_{11} + G_{22}) - F_{11} G_{11} + F_{22} G_{22} \}. \quad (6)$$

By  $F_{ijk}$ ,  $F_{ij}$  we denote the coefficients of the function's  $F(z_1, z_2)$  monomials  $z_i z_j z_k$ ,  $z_i z_j$  correspondingly. Similarly, indices  $G_{ij}$ ,  $G_{ijk}$  denote the coefficient of the second and third order monomials of the function  $G(z_1, z_2)$ .

A passage to the canonical variables  $(z_1, z_2)$  can be attained by the unified transformation. If the relations (3)–(4) are satisfied, then, rewriting (3) in the coordinates  $y_1 = U - U_1$ ,  $y_2 = W$ , we get the following system:

$$\Delta(U) \frac{d}{d\xi} \begin{pmatrix} y_1 \\ y_2 \end{pmatrix} = \begin{pmatrix} 0 & \epsilon \mu \\ -\epsilon \nu & 0 \end{pmatrix} \begin{pmatrix} y_1 \\ y_2 \end{pmatrix} + \begin{pmatrix} \Phi_1(y_1, y_2) \\ \Phi_2(y_1, y_2) \end{pmatrix}, \quad (7)$$

where

$$\epsilon = \begin{cases} +1 & \text{if } \Delta(U_1) > 0, \\ -1 & \text{if } \Delta(U_1) < 0, \end{cases}$$

$$\Phi_1(y_1, y_2) = \varkappa n U_1^{n-2} y_1 y_2 \left( U_1 + \frac{n-1}{2} y_1 \right) + O(|y_i|^4), \quad (8)$$

$$\Phi_2(y_1, y_2) = -\frac{1}{2} y_1^2 (2\dot{\varphi}(U_1) + \ddot{\varphi}(U_1) y_1) - \varkappa n U_1^{n-2} y_2^2 (U_1 + (n-1)y_1) + y_1 y_2 + O(|y_i|^4).$$

In order to pass to the standard representation, we apply the change of coordinates:

$$\begin{pmatrix} z_1 \\ z_2 \end{pmatrix} = \begin{pmatrix} -\epsilon\sqrt{\nu} & 0 \\ 0 & \sqrt{\mu} \end{pmatrix} \cdot \begin{pmatrix} y_1 \\ y_2 \end{pmatrix}.$$

This gives us the system (5), with

$$\begin{aligned} F(z_1, z_2) &= \frac{\varkappa n U_1^{n-2}}{\Omega} z_1 z_2 \left[ \sqrt{\nu} U_1 - \epsilon \frac{n-1}{2} z_1 \right] + O(|z_i|^4), \\ G(z_1, z_2) &= \frac{\mu}{2\nu\Omega} z_1^2 \left[ \epsilon \ddot{\varphi}(U_1) z_1 - 2 \dot{\varphi}(U_1) \sqrt{\nu} \right] - \epsilon \frac{\sqrt{\mu}}{\Omega} z_1 z_2 - \\ &\quad - \frac{\varkappa n U_1^{n-2}}{\Omega} z_2^2 \left[ U_1 \sqrt{\nu} - \epsilon (n-1) z_1 \right] + O(|z_i|^4). \end{aligned} \quad (9)$$

The real part of the Floquet index is easily calculated from (9):

$$\Re C_1 = -\frac{1}{16\Omega} G_{12} (G_{11} + G_{22}) = -\epsilon \frac{1}{16\Omega^2 |\varphi(U_1)|} \left\{ |\Delta(U_1)| \dot{\varphi}(U_1) + \varkappa n |\varphi(U_1)| U_1^{n-1} \right\}. \quad (10)$$

The above can be summarized in the form of the following statement.

**Theorem 1.** *If  $\Delta(U_1) \cdot \psi(U_1) > 0$ , and*

$$|\Delta(U_1)| \dot{\varphi}(U_1) + \varkappa n |\varphi(U_1)| U_1^{n-1} > 0, \quad (11)$$

*then in vicinity of the critical value of the wave pack velocity  $V_{cr1} = U_1$  a stable limit cycle appears.*

## 4 Study of the stationary point $(U_0, 0)$

Rewriting (3) in the coordinates  $X = U - U_0$ ,  $W$  we obtain the system

$$\begin{aligned} \Delta(U_0 + X) \dot{X} &= \Delta(U_0 + X) W, \\ \Delta(U_0 + X) \dot{W} &= [(U_1 - U_0) - X] X^m \psi(U_0 + X) - \\ &\quad - \varkappa n (U_0 + X)^{n-1} W^2 + (U_0 - V + X) W, \end{aligned} \quad (12)$$

where  $\Delta(U_0 + X) = \varkappa [(U_0 + X)^n - \alpha D^2]$ . Our aim is to determine the conditions ensuring that the stationary point  $X = W = 0$  is a topological saddle, or, at least, contains a saddle sector in the right half-plane. The standard theory [22] can be applied for this purpose. Our system can be written down in the form

$$\frac{d}{dT} \begin{pmatrix} X \\ W \end{pmatrix} = \begin{pmatrix} 0 & \Delta(U_0) \\ A & U_0 - V \end{pmatrix} \begin{pmatrix} X \\ W \end{pmatrix} + \text{nonl. terms}, \quad (13)$$

where  $\frac{d}{dT} = \Delta(U_0 + X) \frac{d}{d\xi}$ ,

$$A = \begin{cases} (U_1 - U_0) \psi(U_0), & \text{if } m = 1, \\ 0, & \text{if } m \geq 2. \end{cases}$$

The linearization matrix of the system (13) is nonsingular if  $m = 1$  and the point  $U_*$  lies outside the segment  $[U_0, U_1]$ . In this case the stationary point  $(0, 0)$  is a simple saddle and the homoclinic trajectory corresponds to the solitary wave solution. Out of this case, the Jacobi matrix has at least one zero eigenvalue. To study the behavior of dynamical system in vicinity of a degenerated stationary point, we use the results from [22]. Since we are interested in the case when the trace of the Jacobi matrix is nonzero, the analysis prescribed in Chapter IX of [22] is the following.

1. Find the change of variables  $(U, X, T) \mapsto (x, y, \tau)$  enabling to write down the system (13) in the standard form

$$\frac{dx}{d\tau} = P_2(x, y),$$

$$\frac{dy}{d\tau} = y + Q_2(x, y),$$

where  $P_2(x, y), Q_2(x, y)$  are polynomials of degree 2 or higher.

2. Solve the equation  $y + Q_2(x, y) = 0$  with respect to  $y$ , presenting the result in the form of the decomposition  $y = a_1 x^{\mu_1} + a_2 x^{\mu_2} + \dots$
3. Find the asymptotic decomposition

$$P_2(x, y(x)) = \Delta_m x^m + \dots$$

4. Depending on the values of  $m$  and the sign of  $\Delta_m$ , select the type of the complex stationary point, using the theorem 65 from [22].
5. Return to the original variables  $(U, X, T)$  and analyze whether the geometry of the problem allows for the homoclinic bifurcation appearance.

So let us present the results obtained for the system (12). First we assume, that  $m > 1$ , the statements of the Andronov-Hopf theorem are fulfilled and the point  $U_*$  satisfying the equation  $\Delta(U_*) = 0$  lies outside the segment  $[U_0, U_1]$ , when the parameter  $V$  reaches the second bifurcation value  $V_{cr_2}$ , corresponding to the homoclinic bifurcation. Here we have three possibilities.

- $U_* > U_1$  when the Andronov-Hopf bifurcation occurs (i.e.  $V = V_{cr_1}$ ). This inequality does not change up to the homoclinic bifurcation, when  $V = V_{cr_2} > V_{cr_1}$ .
- The inequalities  $U_0 < U_* < U_1$  take place when  $V = V_{cr_1}$  and the inequality changes for  $U_* < U_0$  when  $V$  belongs to a small neighborhood of  $V_{cr_2} < V_{cr_1}$ .
- $U_* < U_0$  when the Andronov-Hopf bifurcation occurs (i.e.  $V = V_{cr_1}$ ). This inequality does not change up to the homoclinic bifurcation, when  $V = V_{cr_2} < V_{cr_1}$ .

**Remark 1.** *Let us note that in the first case the functions  $\Delta(U)$  and  $\psi(U)$  are negative when  $U \in [U_0, U_1]$ . In the third case both of the functions are positive within the given interval. In the second case  $\psi(U_0)$  is positive, and the factor  $\Delta(U_0)$  changes the sign from negative to positive as  $U_*$  becomes less than  $U_0$ .*

For  $m > 1$ , the canonical system is obtained by the formal change  $(X, W) \mapsto (x, y)$ , and passage to the new independent variable  $\tau = (U_0 - V) T$ , in each of the above cases. As a result of such transformation, we get the following system:

$$\begin{aligned} \frac{dx}{d\tau} &= \frac{\Delta(U_0+x)}{U_0-V} y, = P_2(x, y), \\ \frac{dy}{d\tau} &= y - \frac{1}{V-U_0} \{xy - \varkappa n (U_0 + x)^{n-1} y^2 + x^m [(U_1 - U_0) - x] [\psi(U_0) + \psi'(U_0)x + \dots]\} = \\ &= y + Q_2(x, y). \end{aligned} \tag{14}$$

Presenting  $y$  in the form of series  $y = a_1 x^{\mu_1} + a_2 x^{\mu_2} + \dots$  and solving the equation  $y + Q_2(x, y) = 0$ , we obtain

$$y = a_m x^m + \dots = \frac{U_1 - U_0}{V - U_0} \psi(U_0) x^m + \dots \tag{15}$$

Inserting the function  $y(x)$  into the RHS of the first equation, we get

$$P_2(x, y(x)) = -\frac{\Delta(U_0)}{(U_0 - V)^2} (U_1 - U_0) \psi(U_0) x^m + \dots = \Delta_m x^m + \dots \tag{16}$$

Fulfillment of the statements of the Andronov-Hopf theorem implies that  $\Delta(U_1) \psi(U_1) > 0$  when  $V = V_{cr_1}$ . Previously we assumed that function  $\psi(U)$  does not change sign within the segment  $[U_0, U_1]$ . And this is suffice to conclude that the product remains positive, when the parameter  $V$  attains the value  $V_{cr_2}$ , corresponding to the homoclinic bifurcation. It is quite evident for the cases one and three, because the line  $\Delta(U) = 0$  remains on the same side of the segment  $[U_0, U_1]$ . In the case 2 the situation is somewhat different, because  $\Delta(U_0)$  is negative for  $V = V_{cr_1}$ , while the function  $\psi(U_0)$  is positive and remains so when the parameter  $V$  changes. But the singular line  $\Delta(U) = 0$  is located to the left from the point  $(U_0, 0)$  when  $V$  becomes close to  $V_{cr_2}$ , and then, in accordance with the Remark 1, the product  $\Delta(U_0) \psi(U_0)$  is positive, when the homoclinic bifurcation occurs. So the coefficient  $\Delta_m$  in the decomposition (16) is always negative. Basing on the classification given in Ch. IX of [22], it is possible to formulate the following statement.

**Proposition 1.** *Let the statements of the Theorem 1 be fulfilled and the singular line  $\Delta(U) = 0$  lies outside the segment  $[U_0, U_1]$  of the horizontal axis. Then, for  $m \geq 2$  the origin of the system (14) is a topological saddle, having a pair of outgoing separatrices tangent to the vertical axis and the pair of incoming ones tangent to the horizontal axis, when  $m = 2k$ ,  $k = 1, 2, \dots$ . For  $m = 2k + 1$ ,  $k = 1, 2, 3, \dots$ , the stationary point is a saddle-node with two saddle sectors lying in the right half-plane. Two outgoing separatrices of the saddle sector are tangent to the vertical axis while the incoming one is tangent to the horizontal axis.*

In the following, we present the analysis of system's (12) behavior in vicinity of the stationary point  $(0, 0)$ , assuming that  $\Delta(U_0) = 0$  when  $V = V_{cr2}$ . The results of the study occur to depend on whether or not  $U_0$  is equal to zero. But both of these cases can be analyzed simultaneously. We begin with the case  $m > 1$ , for which the canonical system is obtained by the formal change  $(X, W) \mapsto (x, y)$  and passage to the new independent variable  $\tau = (U_0 - V) T$ . As a result, we get the following system:

$$\begin{aligned} \frac{dx}{d\tau} &= \frac{\varkappa}{U_0 - V} \sum_{k=1}^n \frac{n!}{k!(n-k)!} U_0^{n-k} x^k y, = P_2(x, y), \\ \frac{dy}{d\tau} &= y - \frac{1}{V - U_0} \{xy - \varkappa n (x + U_0)^{n-1} y^2 + x^m [x - (U_1 + U_0)] [\psi(U_0) + \psi'(U_0)x + \dots]\} = \\ &= y + Q_2(x, y). \end{aligned} \tag{17}$$

Presenting  $y$  in the form of series  $y = a_1 x^{\mu_1} + a_2 x^{\mu_2} + \dots$  and solving the equation  $y + Q_2(x, y) = 0$ , we convince that the first term of the asymptotic decomposition  $y(x)$  coincides with (15). This is not surprising, since the second equations of the systems (14) and (17) are identical. Inserting the function (15) into the RHS of the first equation of system (17), we get

$$P_2(x, y(x)) = \begin{cases} -n \varkappa U_0^{n-1} \psi(U_0) \frac{U_1 - U_0}{(U_0 - V)^2} x^{m+1} + \dots, & \text{if } U_0 > 0, \\ -\varkappa \psi(0) \frac{U_1}{V^2} x^{n+m} + \dots, & \text{if } U_0 = 0. \end{cases}$$

In the case  $m = 1$  a passage to the canonical system is attained by means of the transformation

$$x = X, \quad y = W + B X, \quad \tau = (U_0 - V) T,$$

where

$$B = \psi(U_0) \frac{U_1 - U_0}{U_0 - V}. \tag{18}$$

In the new variables, our system reads as follows:

$$\begin{aligned} \frac{dx}{d\tau} &= \frac{\varkappa}{U_0 - V} (y - Bx) \sum_{k=1}^n \frac{n!}{k!(n-k)!} U_0^{n-k} x^k, = P_2(x, y), \\ \frac{dy}{d\tau} &= y + \frac{1}{V - U_0} [\varkappa B^2 U_0^{n-1} (n+1) + B + \psi(u_0)] x^2 + \dots = y + Q_2(x, y). \end{aligned} \tag{19}$$

Solving equation  $y + Q_2(x, y) = 0$ , we obtain

$$y = \frac{1}{U_0 - V} [\varkappa B^2 U_0^{n-1} (n+1) + B + \psi(u_0)] x^2 + \dots$$

Inserting function  $y(x)$  into the RHS of the first equation, we finally get

$$P_2(x, y(x)) = \begin{cases} -\varkappa U_0^{n-1} \psi(U_0) \frac{U_1 - U_0}{(U_0 - V)^2} x^2 + \dots & \text{if } U_0 > 0, \\ -\varkappa \psi(0) \frac{U_1}{V^2} x^{n+1} + \dots & \text{if } U_0 = 0. \end{cases}$$



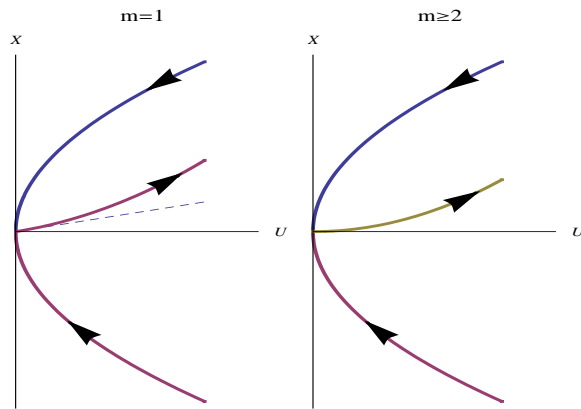


Figure 1: Phase portraits of the system (12) in vicinity of the origin for different values of the parameter  $m$ , in cases when  $U_*(V_{cr_2}) = U_0$

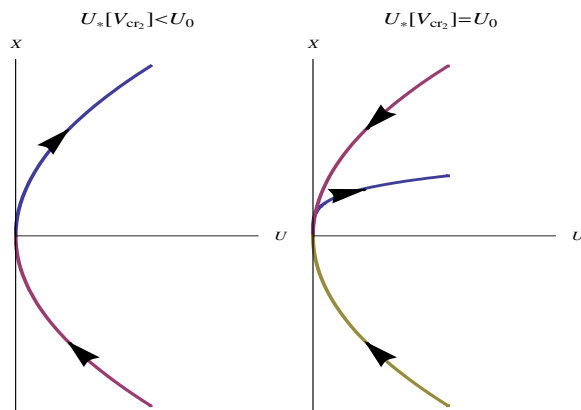


Figure 2: Phase portraits of the system (12) in vicinity of the origin for  $m = 1/2$

So the coefficients of the lowest monomials of the decomposition of  $P_2(x, y(x))$  are negative and the following statement, based on the classification given in [22], holds true for  $U_0 = 0$ .

**Proposition 2.**

1. *If  $m \geq 2$ , and  $m + n$  is an odd natural number, then the origin of the system (17) is a topological saddle having a pair of outgoing separatrices tangent to the vertical axis and the pair of incoming separatrices tangent to the horizontal axis. For even  $m + n$ , the stationary point is a saddle-node with two saddle sectors lying in the right half-plane. Its outgoing separatrices are tangent to the vertical axis while the incoming one is tangent to the horizontal axis. The nodal sector lying in the left half-plane is unstable.*
2. *If  $m = 1$ , and  $n$  is an odd number then the origin of the system corresponding to (19) is a topological saddle identical with that of the previous case. For even  $n$ , the stationary point is a saddle-node identical with that of the previous case.*

Below we formulate the analogous result for  $U_0 > 0$ .

**Proposition 3.** *If  $m = 2k$ ,  $k = 1, 2, \dots$ , then, the origin of the system (17) is a topological saddle having a pair of outgoing separatrices, tangent to the vertical axis and the pair of incoming ones, tangent to the horizontal axis. For  $m = 2k + 1$ ,  $k = 1, 2, \dots$ , the stationary point is a saddle-node with two saddle sectors lying in the right half-plane. Its outgoing separatrices are tangent to the vertical axis while the incoming one is tangent to the horizontal axis. The nodal sector lying in the left half-plane is stable. For  $m = 1$ , and arbitrary  $n \in \mathbb{N}$ , the origin of the system corresponding to (19) is a saddle-node identical with that of the case  $m > 1$ .*

The last case we are going to analyze is that with  $m = \frac{1}{2}$ . The motivation for such a choice will be clear later on. In order to be able to apply the analytical theory, we rewrite the system (12), introducing new variable  $Z = \sqrt{X}$ :

$$\begin{aligned} \frac{dZ}{dT} &= \frac{\varkappa}{2} [\Delta(U_0) + n U_0^{n-1} Z + \dots + Z^{2n-1}] W, \\ \frac{dW}{dT} &= W [(U_0 - V) + Z^2] - \varkappa n [U_0 + Z^2]^{n-1} W^2 + Z [(U_1 - U_0) - Z^2] \psi(U_0 + Z^2). \end{aligned} \tag{20}$$

Let us consider the Jacobi matrix of the system (20), corresponding to the stationary point  $(0, 0)$ :

$$J = \begin{bmatrix} 0 & \frac{\varkappa}{2} \Delta(U_0) \\ \psi(U_0)(U_1 - U_0) & (U_0 - V_{cr2}) \end{bmatrix}. \tag{21}$$

Analysis of the matrix (21) shows, that the origin is a simple saddle when  $U_*(V_{cr2})$  lies outside the segment  $[U_0, U_1]$ . In the case when  $U_*(V_{cr2}) = U_0$ , one of the eigenvalues of the Jacobi matrix is zero, and, in order to classify the stationary point, we use the results from [22]. A passage to the canonical variables is attained by means of the

transformation

$$x = Z, \quad y = W + BZ, \quad \tau = (U_0 - V)T, \quad B = \frac{U_1 - U_0}{U_0 - V} \psi(U_0).$$

The system resulting from this is as follows:

$$\begin{aligned} \frac{dx}{d\tau} &= \frac{\varkappa}{2(U_0 - V)} [nU_0^{n-1}x + \dots + x^{2n-1}] (y - Bx) = P_2(x, y), \\ \frac{dy}{d\tau} &= y - \frac{1}{(V - U_0)} \left\{ B \frac{\varkappa}{2} [nU_0^{n-1}x + \dots + x^{2n-1}] (y - Bx) - \right. \\ &\quad \left. - \varkappa n [U_0 + x^2]^{n-1} - x^3 \psi(U_0) + \dots \right\} = y + Q_2(x, y). \end{aligned} \quad (22)$$

Solving the equation  $y + Q_2(x, y)$  with respect to  $y$  we obtain a series  $y = a_2 x^2 + \dots$ . An outlook of this series' coefficients proves to be unimportant, because they do not contribute to the lowest term of the asymptotic decomposition of the function  $P_2(x, y(x))$ , which is as follows:

$$P_2(x, y(x)) = \begin{cases} -\frac{\varkappa n U_0^{n-1} (U_1 - U_0) \psi(U_0)}{2(U_0 - V)^2} x^2 + \dots, & \text{if } U_0 > 0 \\ -\frac{\varkappa \psi(0)}{2V^2} x^{2n} + \dots, & \text{if } U_0 = 0. \end{cases}$$

Let us formulate the result obtained as the following statement.

**Proposition 4.** *If  $m = 1/2$ , then, in case, when  $U_*(V_{cr_2})$  lies outside the segment  $[U_0, U_1]$ , the origin of the system (22) is a simple saddle. In case when  $U_*(V_{cr_2}) = 0$ , the origin of the system (22) is a saddle-node, having two saddle sectors lying in the right half-plane. Its outgoing separatrices are tangent to the vertical axis while the incoming separatrix is tangent to the horizontal axis.*

The crucial fact appearing from this analysis is that the stationary points  $(0, 0)$  of the canonical systems (17), (19) and (22), depending on the values of the parameters  $m, n$ , are either saddles or saddle-nodes with the saddle sectors placed at the right half-space. The return to the original coordinates does not cause any change in the position of the saddle sectors, but it changes the orientation of vector fields<sup>3</sup> and the angles, at which the outgoing separatrices leave the stationary point. The local phase portraits corresponding to the distinct cases are shown in Fig. 1, reconstructed on the basis of the analysis of the relation between (17)–(19) and the system (12).

Returning to coordinates  $(X, W)$  in the case when  $m = 1/2$ , we obtain the patterns of the phase trajectories shown in Fig. 2. The difference between the case when  $U_*(V_{cr_2}) = U_0$  and when  $U_*(V_{cr_2})$  lies outside the segment  $[U_0, U_1]$  is not essential - in both cases the incoming and outgoing separatrices enter the origin tangent to the vertical axis. Yet, since in the second case the upper separatrix is a mirror image

---

<sup>3</sup>We assume that  $U_0 - V_{cr_2} < 0$ , otherwise the presumable homoclinic loop will not correspond to the wave of "compression". Fulfillment of this condition is verified during the numerical simulation

of the lower one, then one can expect the compactly supported solution to be more symmetric.

Before we start to discuss the results of numerical study of the system (12), let us analyze to what type of solitary waves will correspond the homoclinic loops, presumably appearing in system (3). In order to analyze this issue, we are looking for the asymptotic solution  $W(X) = \alpha_1 X^{\mu_1} + \alpha_2 X^{\mu_2} + \dots$  of the equation

$$\begin{aligned} \Delta(U_0 + X) W \frac{dW}{dX} &= G \equiv \\ &\equiv [(U_0 - V) + X] W - \varkappa n (U_0 + X)^{n-1} W^2 - \psi(U_0 + X) [(U_0 - U_1) + X] X^m, \end{aligned} \quad (23)$$

which is equivalent to the system (12). Let us start with the case  $U_0 = 0$ , for which the equation (23) can be re-written as follows:

$$\begin{aligned} \varkappa X^{n+2\mu_1-1} (\alpha_1 + \alpha_2 X^{\mu_2-\mu_1} + \dots) (\mu_1 \alpha_1 + \mu_2 \alpha_2 X^{\mu_2-\mu_1} + \dots) &= \\ = X^{1+\mu_1} (\alpha_1 + \alpha_2 X^{\mu_2-\mu_1} + \dots) - V X^{\mu_1} (\alpha_1 + \alpha_2 X^{\mu_2-\mu_1} + \dots) - & \quad (24) \\ - \varkappa n X^{n+2\mu_1-1} (\alpha_1^2 + 2\alpha_1\alpha_2 X^{\mu_2-\mu_2} + \dots) - [X^{m+1} + U_1] X^m \psi(0) + \dots \end{aligned}$$

The procedure of solving (24) is pure algebraic: we collect the coefficients of different powers of  $X$  and equalize them to zero. The lowest power in the RHS is either  $X^{\mu_1}$  or  $X^{n+2\mu_1-1}$ . The number  $n + 2\mu_1 - 1$  cannot be less or equal to  $\mu_1$ , because it involves the inequality  $0 < \mu_1 \leq 1 - n$ , which is impossible for any natural  $n$ . On the other hand, if  $n + 2\mu_1 - 1 \leq m$ , then  $\mu_1$  becomes an "orphan" and  $\alpha_1$  should be nullified.

So  $X^{n+2\mu_1-1}$  cannot be the lowest monomial. From this, it immediately appears that the only choice leading to a nontrivial solution is  $\mu_1 = m$ .

For  $U_0 > 0$  the equation is as follows:

$$\begin{aligned} \varkappa X^{2\mu_1} (\alpha_1 + \alpha_2 X^{\mu_2-\mu_1} + \dots) (\mu_1 \alpha_1 + \mu_2 \alpha_2 X^{\mu_2-\mu_1} + \dots) &= \\ = \psi(U_0) X^m [(U_1 - U_0) - X] - & \\ - \varkappa n [U_0^{n-1} + \dots] (\alpha_1^2 X^{2\mu_1} + \dots) + [X + (U_0 - V)] [\alpha_1 X^{\mu_1} + \dots]. \end{aligned} \quad (25)$$

Using the analogous arguments as before for the present (more simple) case, we conclude that  $\mu_1 = m$ .

The decomposition obtained can be used to asymptotically integrate the equation

$$\frac{dX}{d\xi} = W = a_1 X^m + \dots$$

which immediately gives in the lowest order the expression

$$X = \begin{cases} [a_1(1-m)(\xi - \xi_0)]^{\frac{1}{1-m}}, & \text{if } m \neq 1, \\ C \exp[a_1(\xi - \xi_0)], & \text{if } m = 1, \end{cases}$$

from which we conclude that the trajectory reaches the origin in "finite time" if  $m < 1$ .

Unfortunately, in case when  $m \in N_+$ , presented above result cannot be attributed to both of the saddle sector separatrices, forming the closed loop. In fact, the incoming separatrix of the stationary point  $(0, 0)$  in all cases considered here is tangent to the vertical axis and therefore cannot be described by the formula (26) when  $m \geq 1$ . The above formula, then, describes the asymptotic behavior of the "tail" of the solitary wave, corresponding to the homoclinic solution.

To complete the analysis, we resort to some arguments, concerning the other end of the homoclinic trajectory. It is the common feature of almost all the cases considered here, that the incoming separatrix is tangent to the vertical axis, with the exception of the case when  $m = 1$  and  $U_*(V_{cr2})$  lies outside the interval  $(U_0, U_1)$ . This enables us to assume that in vicinity of the origin  $W = -BU^\sigma + o(U^\sigma)$ , where  $0 < \sigma < 1$  and  $B > 0$ . An approximate equation describing the first coordinate of the separatrix is, then, as follows

$$\frac{dU}{d\xi} = -BU^\sigma + o(U^\sigma).$$

Performing the asymptotic integration, we obtain, up to the change of notation, the solution identical with (26), concluding from this that in all analyzed above cases with  $m, n \in N_+$ , the incoming separatrix reaches the origin in finite "time".

It is obvious, that similar arguments can be applied to the analysis of presumable homoclinic trajectory, corresponding to  $m = 1/2$ . It appears from the above analysis, that the incoming and outgoing separatrices are tangent to the vertical axis and both of them reach the origin in finite "time". Let us note that when  $U_*(V_{cr2})$  lies outside  $[U_0, U_2]$ , the asymptotic behavior of the separatrices is described by the formula

$$X = \pm \sqrt{\gamma(\xi - \xi_0)}, \quad \gamma > 0.$$

So this is the only case when the homoclinic trajectory corresponds with certain to the compactly supported solution of the equation (1).

## 5 Results of numerical simulation

Since the parabolic case was discussed in detail in our previous work [19], we mainly concentrate here on the hyperbolic case, corresponding to  $\alpha > 0$ . Numerical simulations of the system (12) were carried out with  $\varkappa = 1$ ,  $U_1 = 3$ ,  $U_2 = 1$ . The remaining parameters varied from one case to another. The results of qualitative study evidence that, within the variety of parameters that were analyzed, the only case when the homoclinic loop corresponds to the compactly supported solution is that with  $m = 1/2$ . We discuss the results concerning the details of the phase portraits in terms of the reference frame  $(X, W)$ . The numerical experiments show that in case when  $m = 1/2$ ,  $n = 1$  and  $U_*(V_{cr2}) < U_0$ , both of the separatrices forming closed loop enter the stationary point  $(0, 0)$  tangent to the vertical axis, Fig. 3, the left picture. The right picture shows the compactly supported solution to Eq. (1), corresponding to the closed loop. When  $U_*(V_{cr2})$  tightly approaches  $U_0$ , no matter from the left or from the right, the left side of the homoclinic trajectory is clasped to the vertical axis, Fig. 4,

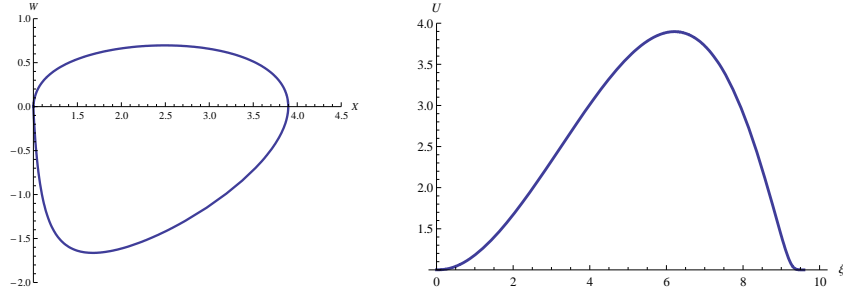


Figure 3: Homoclinic solution of the system (12) with  $\varphi(U_0 + X) = X^{1/2}$  (left) and the corresponding compactly supported TW solution to Eq. (1) (right), obtained for  $n = 1$ ,  $\alpha = 0.12$ ,  $V_{cr2} \cong 2.68687$  and  $U_* - U_0 = -0.133684$

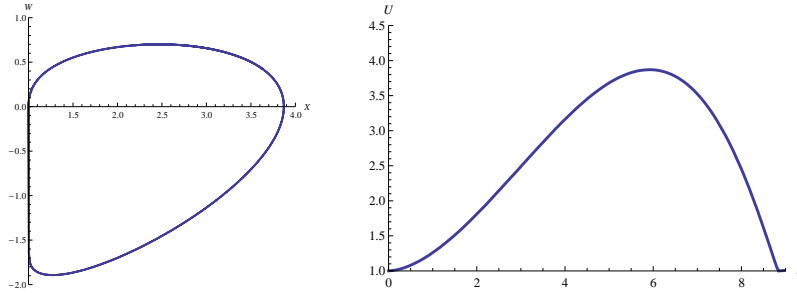


Figure 4: Homoclinic solution of the system (12) with  $\varphi(U_0 + X) = X^{1/2}$  (left) and the corresponding TW solution to Eq. (1) (right), obtained for  $n = 1$ ,  $\alpha = 0.13827$ ,  $V_{cr2} \cong 2.68892$  and  $U_* - U_0 = 0.99973$

left. The corresponding compactly supported solution has more sharp front, Fig. 4, right.

As it was shown in the previous section, appearance of the soliton-like solutions is possible merely in case when  $m = 1$ . In accordance with the predictions of our qualitative analysis, such solutions were observed for  $m = n = 1$  and values of the parameters guaranteeing the fulfillment of the inequality  $U_*(V_{cr2}) < U_0$ . As it is seen on the left picture of Fig. 5, both of the separatrices of the saddle sector form nonzero angle with the vertical axis and this gives us the reason to state that the homoclinic loop corresponds in this case to the smooth solitary wave, which is nonzero for any  $\xi \in R$ .

When  $U_*$  tightly approaches  $U_0$ , the incoming separatrix of the homoclinic trajectory is clasped to the vertical axis (Fig. 6, left) and the solutions reminding shock waves with relaxed tails are observed in place of soliton-like wave packs (Fig. 6, center, right).

For  $m \geq 2$  merely the shock-like solutions have been observed in numerical experiments. This confirms the arguments put forward in the previous section. The outlook of the TW occurs to depend on the values of the parameters  $m, n$ . A series of shock-like

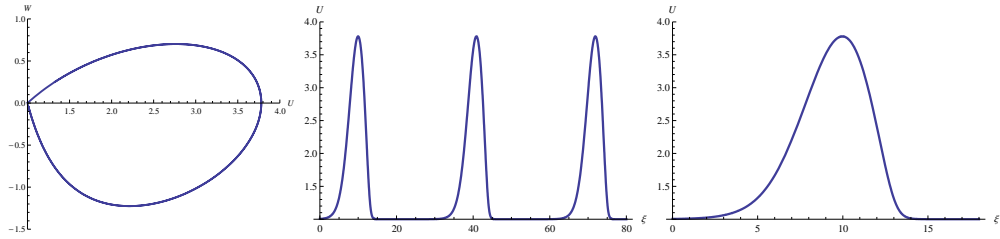


Figure 5: Homoclinic solution of the system (12) with  $\varphi(U_0 + X) = X^1$  (left), the corresponding tandem of well-localized soliton-like solutions to Eq. (1) (center), and the soliton-like solution (right), obtained for  $n = 1$ ,  $\alpha = 0.06$ ,  $V_{cr2} \cong 2.65795$  and  $U_* - U_0 = -0.576119$

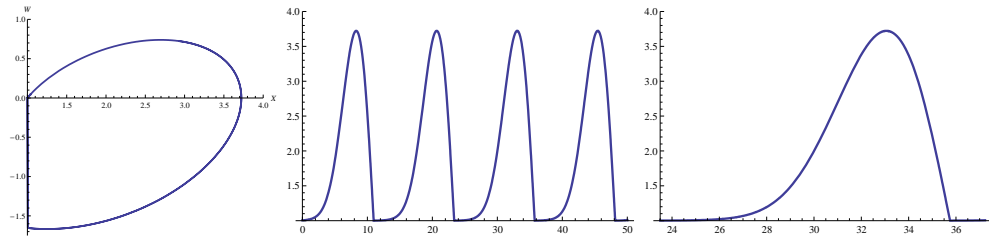


Figure 6: Homoclinic solution of the system (12) with  $\varphi(U_0 + X) = X^1$  (left), the corresponding tandem of solitary wave solutions to Eq. (1) (center) and a single solitary wave solution (right), obtained for  $n = 1$ ,  $\alpha = 0.142$ ,  $V_{cr2} \cong 2.65489$  and  $U_* - U_0 = 0.000878617$

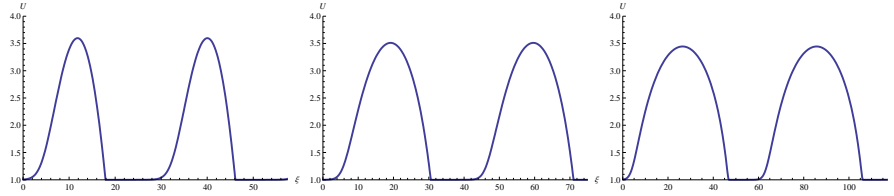


Figure 7: Tandems of shock-like solutions to Eq. (1), corresponding to  $\varphi(U_0 + X) = X^1$ ,  $U_* \approx U_0$ ,  $n = 2$  (left),  $n = 3$  (center), and  $n = 4$  (right)

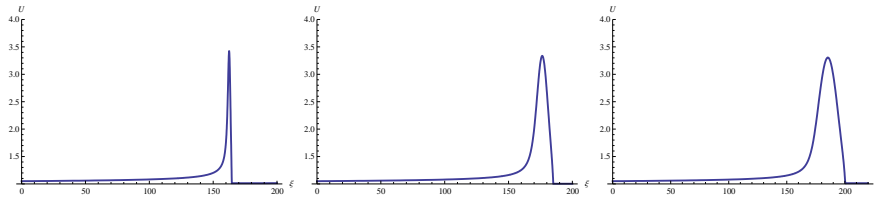


Figure 8: Shock-like solutions to Eq. (1), corresponding to  $\varphi(U_0 + X) = X^3$ ,  $U_* \approx U_0$ ,  $n = 1$  (left),  $n = 3$  (center), and  $n = 4$  (right)

solutions corresponding to  $m = 1$  and  $n = 2, 3, 4$  are shown in Fig. 7. It is seen, that effective width of the TW grows as  $n$  grows, and the shape becomes more and more gently sloping.

The next series (Fig. 8) shows the TW corresponding to  $m = 3$  and  $n = 1, 2, 3$ . This picture differs from the previous one in that the "tails" of the travelling waves are longer. A common feature of all the cases with  $m \geq 2$  is the strong stability of the equilibrium, especially in the direction of the outgoing separatrix. Choosing the initial data more and more close to the origin, we are able to elongate the "tail" without limit. Besides, the profiles of the TW become more and more smooth as the  $n$  grows.

Fig. 9 shows the series obtained for  $n = 4$  and  $m$  varying from 1 to 3. It is seen that the waves become more and more localized as the parameter  $m$  grows. This series mainly characterizes the growing stability of the saddle point  $(0, 0)$ .

Finally, let us discuss what happens when  $U_*(V_{cr1}) > U_1$ . The birth of the stable limit cycle is possible in this case, if  $\varphi(U) < 0$ . Therefore we use in numerical ex-

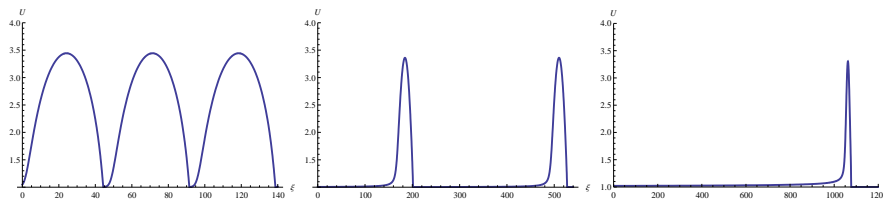


Figure 9: Shock-like solutions to Eq. (1), corresponding to  $\varphi(U_0 + X) = X^m$ ,  $U_* \approx U_0$ ,  $n = 4$ ,  $m = 1$  (left),  $m = 2$  (center), and  $m = 3$  (right)



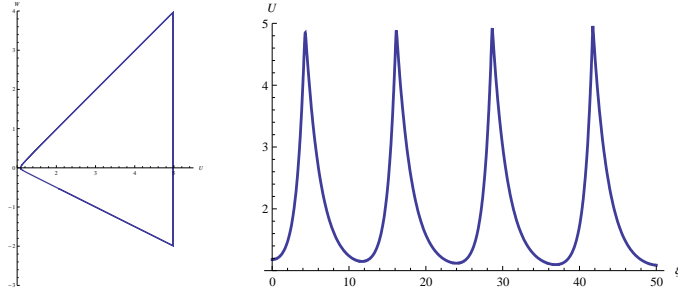


Figure 10: Periodic solution of the system (12) with  $\varphi(U_0 + X) = -X^1$  (left) and the corresponding tandem of generalized cusp-like solutions to Eq. (1) (right), obtained for  $n = 1$ ,  $\alpha = 0.552$ ,  $V_{cr2} \cong 3.00593$  and  $U_* - U_1 = 1.98765$

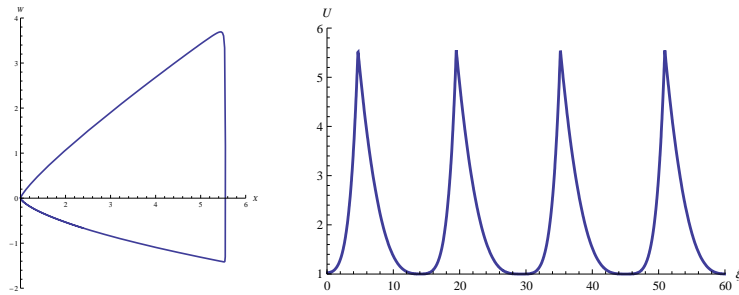


Figure 11: Homoclinic solution of the system (12) with  $\varphi(U_0 + X) = -X^{\frac{1}{2}}$  (left) and the corresponding tandem of generalized cusp-like solutions to Eq. (1) (right), obtained for  $n = 1$ ,  $\alpha = 0.562$ ,  $V_{cr2} \cong 3.14497$  and  $U_* - U_1 = 2.55863$

periment the function  $\varphi(U_0 + X) = -X^m$ . Numerical study shows, that the radius of the limit cycle grows as the bifurcation parameter  $V$  grows. Simultaneously the coordinate  $U_*(V)$  of the singular line intersection with the horizontal axis moves to the right, but not so quickly as the radius of the limit cycle. In most cases the destruction of the periodic trajectory observed was due to its interaction with the line  $\Delta(U) = 0$ . For  $m = n = 1$  we succeeded in observing how the limit cycle approaches the line of singularity, attaining the triangle shape Fig. 10, left. The corresponding succession of the cusp-like travelling waves is shown in the right picture. Let us note, that we were not able to follow the moment of the homoclinic bifurcation, varying the parameters  $\alpha$  and  $V$ .

Experimenting with  $m = 1/2$ ,  $n = 1$  occurs to be more easy. The homoclinic bifurcation, shown in the left picture of the Fig.10, takes place when the far end of the cycle attains the line  $\Delta(U) = 0$ . The presence of the singular line causes a drastic change of the shape of homoclinic loop, which equally well can be called the "homoclinic triangle". The right picture shows the corresponding succession of the well-separated peakons.

Let us note in conclusion that numerical experiments performed for the parabolic case, i.e. for  $\alpha = 0$ , demonstrate quite similar behavior of the TW and their dependence upon the parameters (for more details, see [19]).

## 6 Final remarks

So it was shown in this study, that the generalized convection-reaction-diffusion equation (1) possesses a wide variety of TW solution, such as solitons, compactons, shock-like solutions and peakons. The result of the qualitative analysis and numerical simulation are in agreement with each other. The hyperbolic case occurs to be more reach, since the soliton-like solutions and peakons are observed only when  $\alpha > 0$ . Surprisingly enough, one-sided compactons exist not only when the stationary point lies on the singular line  $\Delta(U) = 0$ , but also when it lies left-hand side of it. Condition  $m > 1$  assures in the last case the existence of the sharp front.

The results obtained are not rigorous. Only heuristic arguments are attached in favor of the statement that for  $m \neq 1/2$  an infinite "time" is needed to reach the point  $(U_0, 0)$ , moving along the incoming separatrix of the saddle sector. The precision of the numerical method used does not enable us to get convinced that we deal with shock fronts with exponentially localized "tails" in cases of small  $m \in N_+$ , when the critical point  $(U_0, 0)$  demonstrates essential instability and the "trains" of sharply ended pulses are observed, instead of truly localized solitary waves. More precise description of the wave patterns seems to be possible by presenting them in the form of exponential series [13]. Another possibility is connected with the application of the rigorous computing methods [23]. Aside of the scope of this study remained the study of stability and attracting properties of the invariant TW solutions. We plan to address these issues in the forthcoming studies.

## References

- [1] Olver P., *Applications of Lie Groups to Differential Equations*, Springer-Verlag: New York, Berlin, Tokyo, 1996.
- [2] Dodd R.K., Eilbek J.C., Gibbon J.D., Morris H.C., *Solitons and Nonlinear Wave Equations*, Academic Press, London 1984.
- [3] W.Fickett, Davis W.C., *Detonation*, Berkley: Univ. of California Press, 1979.
- [4] Rosenau P. and Hyman J., *Compactons: Solitons with Finite Wavelength*, Phys Rev. Letter, vol. 70 (1993), No 5, 564-567.
- [5] Li Y.A. and Olver P.J., *Convergence of Solitary-Wave Solutions in a Perturbed Bi-Hamiltonian Dynamical System. 1. Compactons and Peakons*, Discrete and Continuous Dynamical systems, vol. 3 (1997), pp. 419-432. (see also <http://www.math.umn.edu/~olver>)
- [6] Li Y.A. and Olver P.J., Rosenau Ph., *Non-Analtic Solutions of Nonlinear Wave Models*, in: nonl. Theory of Generalized functions, M. grosser, G. Hormann, M. Kunzinger and M. Oberguggenberger, eds., Research Notes in Mathematics, vol. 401, Chapman and hall/CRC, New York, 1999, pp. 129-145 (see also <http://www.math.umn.edu/~olver>).
- [7] Vladimirov V., *Compacton-like Solutions of the Hydrodynamic System Describing Relaxing Media* , Rep. Math. Phys. 61 (2008), 381-400.
- [8] Joseph D.D., Preziosi, L., *Heat Waves*, Review of Modern Physics, vol. 61, no. 1 (1989), 41-73.
- [9] Makarenko A.S., *New Differential Equation Model for Hydrodynamics with Memory Effects*, Reports on Mathematical Physics, vol. 46, No. 1/2 (2000), 183-190.
- [10] Makarenko A.S., Moskalkov M., Levkov S., *On Blow-up Solutions in Turbulence*, Phys Lett., vol. A23 (1997), 391-397.
- [11] Kar S., Banik S.K., Ray Sh., *Exact Solutions of Fisher and Burgers Equations with Finite Transport Memory*, Journal of Physics A: Mathematical and Theoretical, vol. 36, No. 11 (2003), 2771-2780.
- [12] Vladimirov V. and Kutafina E., *Exact Travelling Wave Solutions of Some Non-linear Evolutionary Equations* , Rep. Math. Physics, vol. 54 (2004), 261-271.
- [13] Vladimirov V. and Kutafina E., Pudelko A., *Construction Soliton and Kink Solutions of PDE Models in Transport and Biology*, SIGMA, vol. 1 (2005), Paper 16.

- [14] Vladimirov V. and Kutafina E., *Analytical Description of the Coherent Structures within the Hyperbolic Generalization of Burgers Equation*, Rep. Math. Physics, vol.58 (2006), 465.
- [15] Vladimirov V. and Maczka Cz., *Exact Solutions of Generalized Burgers Equation, Describing Travelling Fronts and Their Interactions* , Rep. Math. Physics, vol. 60 (2007), 317-328.
- [16] Fahmy E.S., Abdusalam h.A., Raslan K.R., *On the Solutions of the Time Delayed Burgers Equation*, Nonlinear Analysis, vol. 69 (2008), 4475-4786.
- [17] Rosenau P. and Pikovsky A., *Phase Compactons in Chains of Dispersively Coupled Oscillators*, Phys. Rev. Lett., vol. 94 (2005) 174102.
- [18] Pikovsky A. and Rosenau P., *Phase Compactons*, Physica D, vol. 218 (2006) 56–69.
- [19] Vladimirov V., Maczka Cz., *On the Localized Wave Patterns Supported by Convection–Reaction–Diffusion Equation* , Rep. Math. Physics, (2009), to appear.
- [20] Hassard B., Kazarinoff N., Wan Y.-H., *Theory and Applications of Hopf Bifurcation*, Cambridge Univ. Press: London, New York, 1981.
- [21] Guckenheimer J., Holmes P., *Nonlinear Oscillations, Dynamical Systems and Bifurcations of Vector Fields*, Springer–Verlag: New York Inc, 1987.
- [22] Andronov A., Leontovich E., Gordon I and Meyer A., *Qualitative Theory of 2-nd Order Dynamical Systems*, Nauka Publ., Moscow, 1976 (in Russian).
- [23] Mishaikov K., Zgliczynski P., *Rigorous Numerics for PDEs:the Kuramoto-Sivashinski Equation*, Foundations of Computational mathematics, vol. 1 (2001), 255-288.